Chapter 5

Simulation Results

The TFDTLM scheme was found to have improved dispersion characteristics as compared to the SSCN and HSCN. This conclusion can in fact be generalized to any general time domain TLM scheme. The main advantage of the TFDTLM is its ability to model inhomogeneous as well as frequency dispersive material parameters more directly and more accurately than existing TDTLM schemes.

For the purpose of verification, the TFDTLM was implemented in a three dimensional TLM node . The scattering matrix was derived, as was shown in chapter 2, in terms of the normalized characteristic impedance of the link lines. The connection procedure was implemented as shown in equations (3.19) and (3.20).

5.1 Simulation of a resonant cavity

A cavity of size 5 cm x 5 cm x 5 cm was simulated with a uniform grid of ten cells in each coordinate direction. A comparison with the type II time domain HSCN is performed in two cases. In the first case, the cavity was filled was a lossless dielectric with a relative dielectric constant of 5. The resonance frequencies were calculated in the TFDTLM approach and the HSCN and compared to the actual or theoretical values. In the second case, some losses are introduced to the dielectric filling of the cavity and the quality factor is calculated for the HSCN and the TFDTLM approach and compared with the theoretical values.

The filter coefficients in the TFDTLM were optimized up to a frequency where the maximum cell dimension is in the order of 0.18 times the wavelength in a medium with $\varepsilon_r = 5$. This range is guaranteed to cover the frequency range over which the TLM is always operated for a given cell dimension. Usually the cell dimension in a TLM node would be chosen to be less than 0.1 times the corresponding wavelength at the maximum frequency of interest.

Figure (5.1a-b) compare the simulation results of type II HSCN and the TFDTLM in modeling a lossless cavity with $\varepsilon_r = 5$. From the Figure, it appears that the behavior of type II HSCN and that of the TFDTLM with a first order filter approximation are almost identical in the low frequency range, up to 3 GHz and are very close to the theoretical values. As the frequency increases, the resonance frequencies obtained from the HSCN start to shift from the actual values whereas the TFDTLM almost maintains the same order of accuracy. The Figure also shows that the resonances provided by the TFDTLM are sharper and much more pronounced than those given by the HSCN at higher frequencies.

Figure (5.2a-b) show a comparison between the accuracy of the type II HSCN and the TFDTLM in simulating the resonances of a lossy cavity with $\sigma = 0.025$ S/m and $\varepsilon_r = 5$. Table 5.1 shows the quality factors calculated from both schemes as compared to the actual values. The results in table 5.1 shows that the TFDTLM can provide improved accuracy in calculating the quality factor and consequently in modeling the losses in the medium. Both the TFDTLM and the HSCN have acceptable order of accuracy in the low frequency, although the TFDTLM is still better. As the frequency increases, the HSCN significantly degrades whereas the TFDTLM maintains almost the same order of accuracy with very slight degradation.

Figure (5.3a-b) show similar results to those in (5.2a-b) but with higher loss tangent or more losses. In this simulation, the conductivity was increased to 0.05 s/m and the dielectric constant is maintained. Table 5.2 compares the error in estimating the quality factor in both

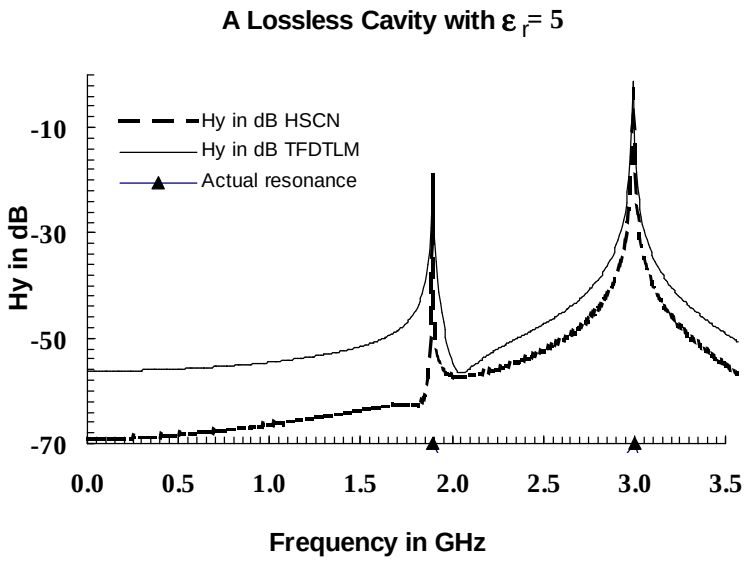

Figure 5.1a Resonance of a 5 cm x 5 cm x cm cavity in the frequency range 0 to 3.5 GHz

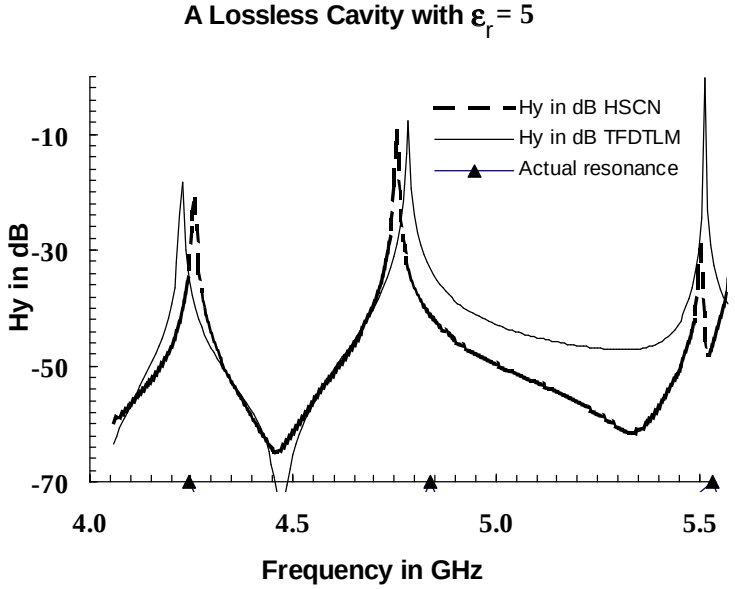

Figure 5.1 b Resonance of a 5 cm x 5 cm x cm cavity in the frequency range 4 to 5.6 GHz

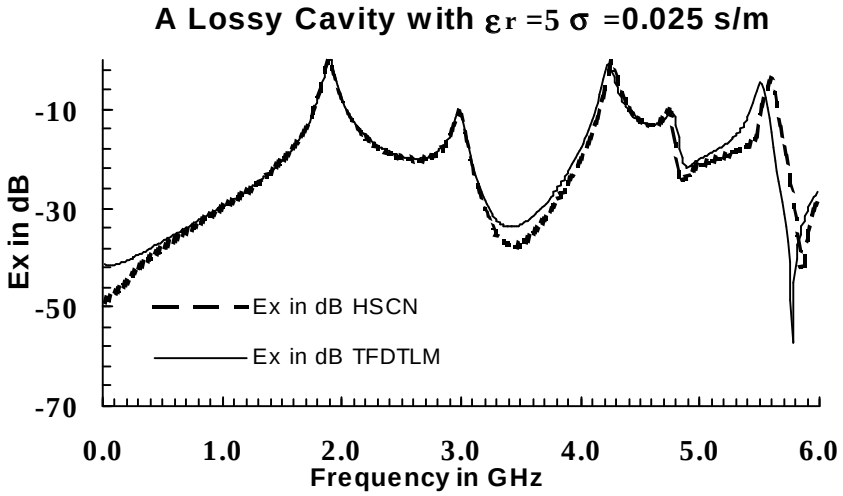

(a)

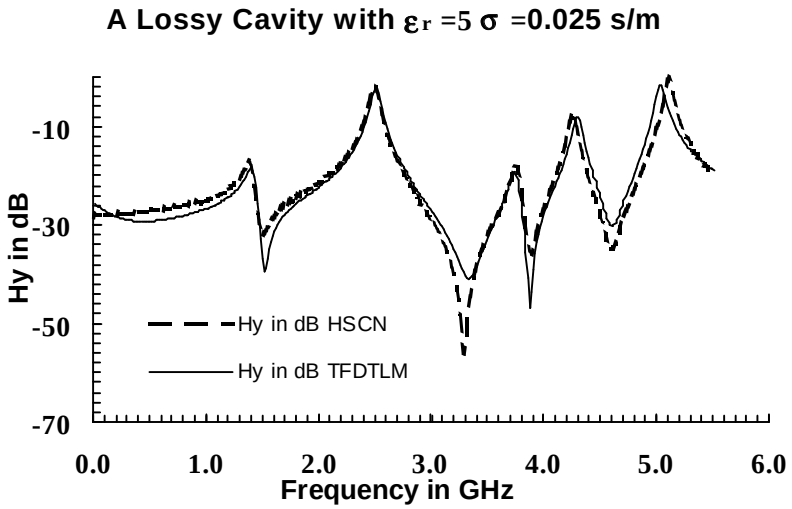

(b)

Figure 5.2 Simulation of a lossy cavity with both type II HSCN and FDTLM
$\varepsilon_r = 5$ $\sigma = 0.025$ s/m a- E_x in dB b- H_y in dB

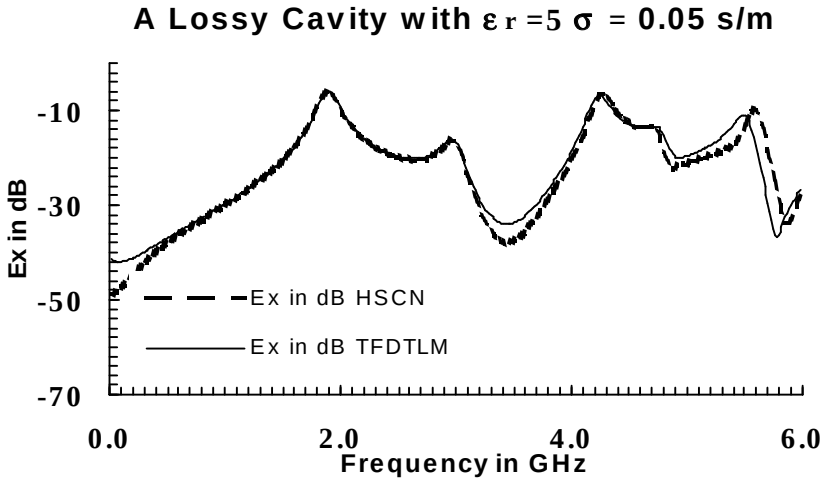

(a)

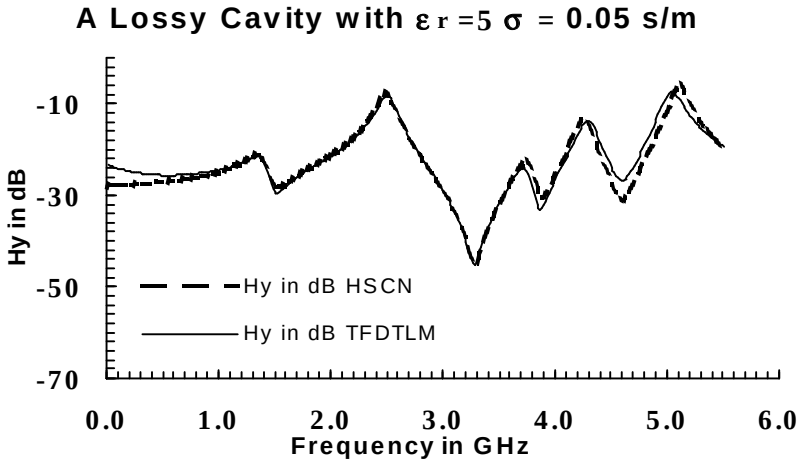

(b)

Figure 5.3 Simulation of a lossy cavity with both type II HSCN and FDTLM
$\varepsilon_r = 5$ $\sigma = 0.05$ s/m a- E_x in dB b- H_y in dB

Table 5.1 comparison of the percentage error in the Q factor estimation obtained from the HSCN and TFDTLM for $\varepsilon_r = 5$ σ = 0.025 s/m

$f_{o\ actual}$	$f_{o\ HSCN\ II}$	$f_{o\ TFDTLM}$	$Q_{HSCN\ II}$	Q_{TFDTLM}	$error_{HSCN}$ HSCN	$error_{TFDTLM}$
1.8974	1.8902	1.8902	21.5	20.79	2.4 %	-0.98 %
3	2.9854	2.9854	34.77	33.02	4.8 %	-0.43 %
4.2426	4.26	4.23	52.77	46.4	11.5 %	-1.25 %
4.8374	4.756	4.786	61.7	53.13	16 %	-0.1 %
5.5317	5.6	5.51	75.4	59.2	21 %	-3 %

Table 5.2 Comparison of the percentage error in the Q factor estimation obtained from the HSCN and TFDTLM for $\varepsilon_r = 5$ σ = 0.05 s/m

$f_{o\ actual}$	$f_{o\ HSCN\ II}$	$f_{o\ TFDTLM}$	$Q_{HSCN\ II}$	Q_{TFDTLM}	$error_{HSCN}$ HSCN	$error_{TFDTLM}$
1.8974	1.8826	1.8976	10.7	10.42	2.4 %	-0.98 %
3	2.9852	2.9852	17.57	16.58	6.1 %	-0.1 %
4.2426	4.237	4.2005	26.7	24.19	13 %	3.4 %
4.8374	4.748	4.78	31.5	27.9	21 %	-5.3 %
5.5317	5.6	5.52	38	29.3	22 %	-3 %

the HSCN and the TFDTLM. The table shows that for twice as much losses, the HSCN is significantly degraded even in the low frequency range. The TFDTLM on the other hand, has maintained almost the same order of accuracy in the relatively low frequency range with slight degradation in the high frequency range.

From the results in tables 5.1 and 5.2, it appears that the traditional time domain TLM overestimates the quality factor or in other words underestimates the losses in the medium. This can also be concluded by observing the time domain response in the time domain TLM. Figures (5.4a-b) shows the time domain response of the e_x field in the HSCN II as compared to the real part of the e_x field versus the number of iteration in the TFDTLM. The Figures clearly indicates that the response in the TFDTLM decays much faster than the HSCN. Figure (5.4 c-d) zoom into the iterations from 2000 to 4000 in the TFDTLM versus the time steps from 2000 to 4000 in the HSCN. The figures shows at the 2000^{th} iteration in the TFDTLM, the real part of e_x has dropped to a value of 10^{-4} relative to an initial value of around 50, it then continues to decay rapidly to a very small level. In the time domain HSCN on the other hand,

the e_x field component at the 2000^{th} time step has a value of about 10% of the initial value. Furthermore, it appears that it continues to oscillate with a maximum magnitude of about 10 % of the initial value. It is worth mentioning that the number of time steps were even increased to 16000 and the electric field component never dropped any further. This explains the under estimated losses obtained by the time domain HSCN.

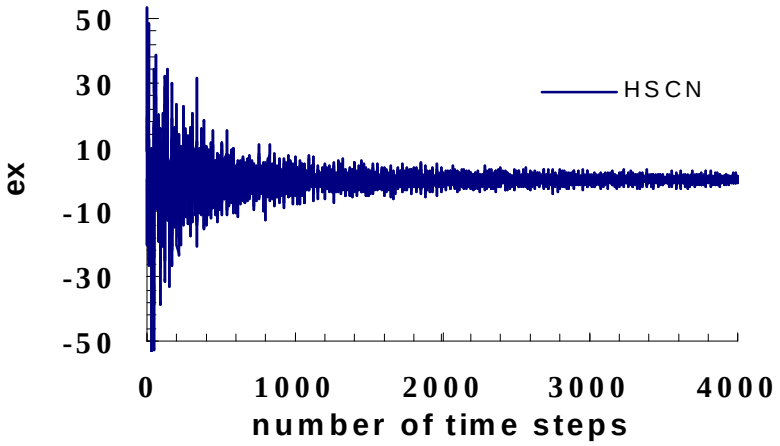

(a)

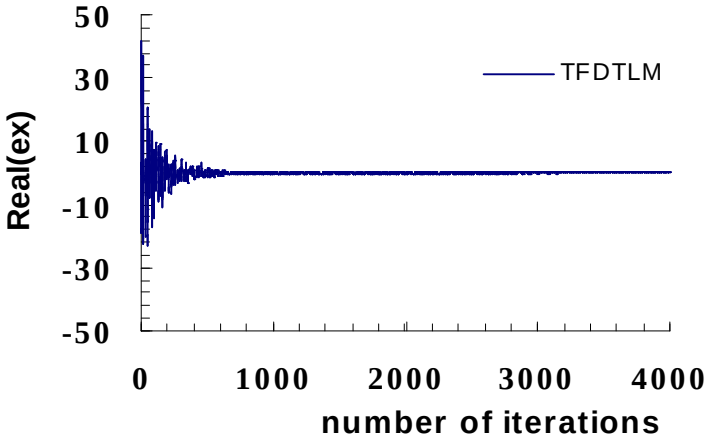

(b)

Figure 5.4 Comparison of the rate of convergence of HSCN II and FDTLM in the simulation of lossy cavity, iterations 1:4000 $\varepsilon_r = 5$ $\sigma = 0.05$ s/m a- HSCN b- TFDTLM

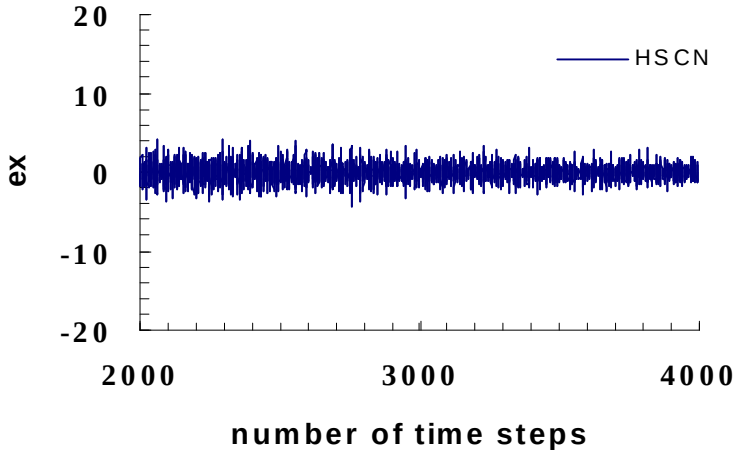

(c)

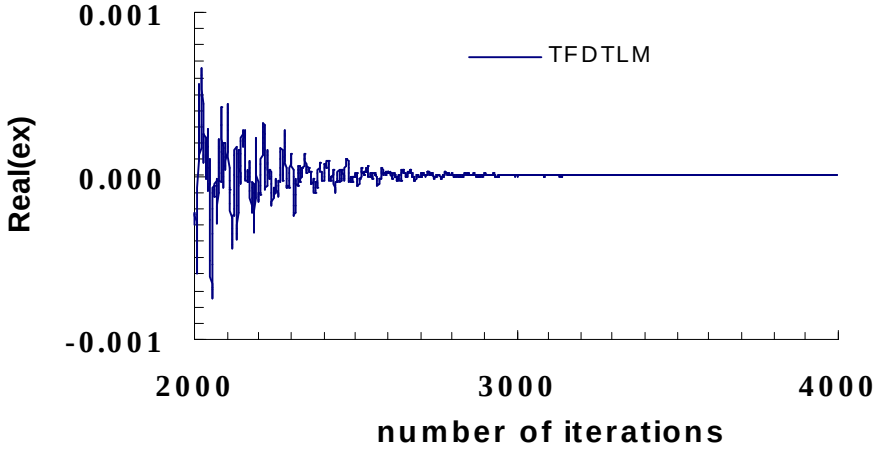

(d)

Figure 5.4 Comparison of the rate of convergence of HSCN II and FDTLM in the simulation of lossy cavity iterations 2000:4000 $\varepsilon_r = 5$ $\sigma = 0.05$ s/m c- HSCN d- TFDTLM

5.2 Simulation of rectangular waveguide structure

In this case, a rectangular waveguide structure is simulated. The dominant TE_{10} mode is excited and the impedance of the dominant mode is calculated from the simulation. The accuracy of the calculated impedance obtained using the HSCN is then compared to that obtained using the TFDTLM for different dielectric constants. The waveguide structure shown in Figure (5.5) has a = b = 5 cm. A section of the waveguide of length 10 cm is considered. A second order Higdon's absorbing boundary condition [26-28] is used as a matched termination at z = 0 and z = 10 cm. The derivation of the boundary equations is shown in Appendix C. In the TFDTLM method, a first order filter approximation is used. The filter is denoted by F_1 and has the form

$$F_1 = e^{-\gamma_1 \Delta l_1}\left(\frac{a_0 + a_1 e^{-\gamma_1 \Delta l_1}}{b_0 + b_1 e^{-\gamma_1 \Delta l_1}}\right) \tag{5.1}$$

Free space is considered the reference medium i.e. $\gamma_1 = j\omega\sqrt{\mu_0 \varepsilon_0}$. A uniform cell is used with dx = dy = dz $= 2\Delta\ell_1$ =0.5 cm. The filter coefficients are optimized in a frequency range where the a maximum cell dimension is less than or equal to 0.125 times the corresponding wavelength.

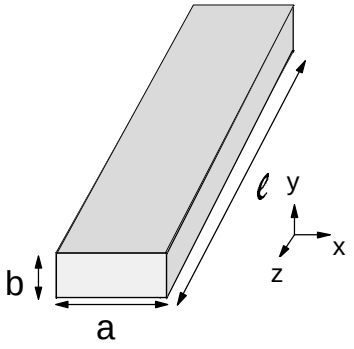

Figure 5.5 A rectangular waveguide structure

Figure (5.6a) compares the magnitude of the impedance of the dominant TE_{10} mode obtained from the traditional time domain TLM to that obtained by the TFDTLM method. the relative dieclectric constant is 2. Figure (5.6b) shows the error in the impedance calculation after cutoff for both the HSCN and the TFDTLM. A frequency range from 1.25 f_c to 2.8 f_c is considered. The Figure shows an improved order of accuracy for the TFDTLM over the traditional time domain TLM. In the frequency range considered, the HSCN has an average magnitude error of about 3.5 % corresponding to only 1.75% for the TFDTLM.

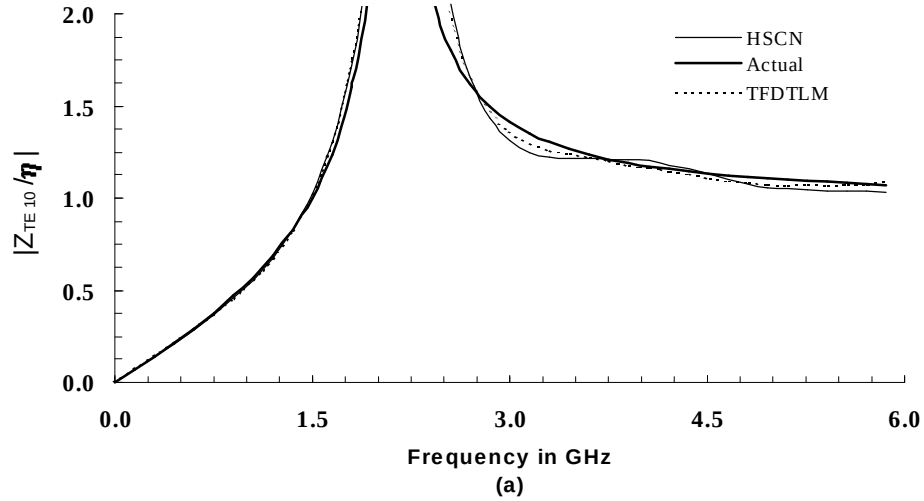

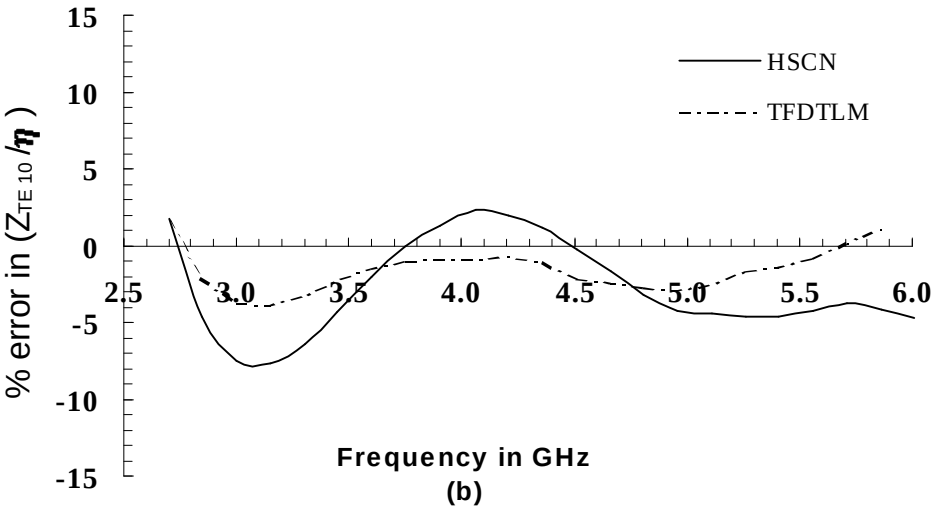

Figure 5.6 Comparison between HSCN II and FDTLM in simulating a rectangular waveguide $\varepsilon_r = 2$ a- $|Z_{TE10}/\eta|$ b- % error in Z_{TE10}/η after cutoff

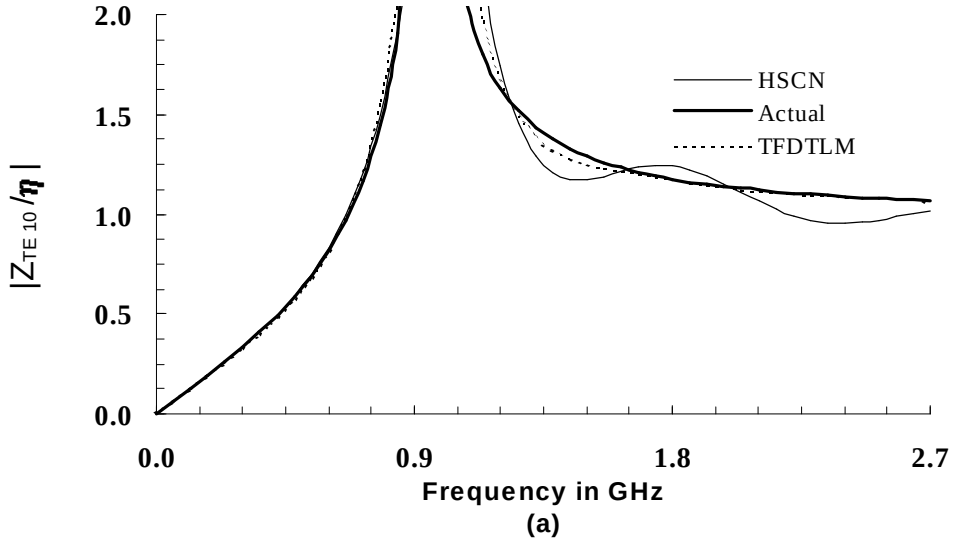

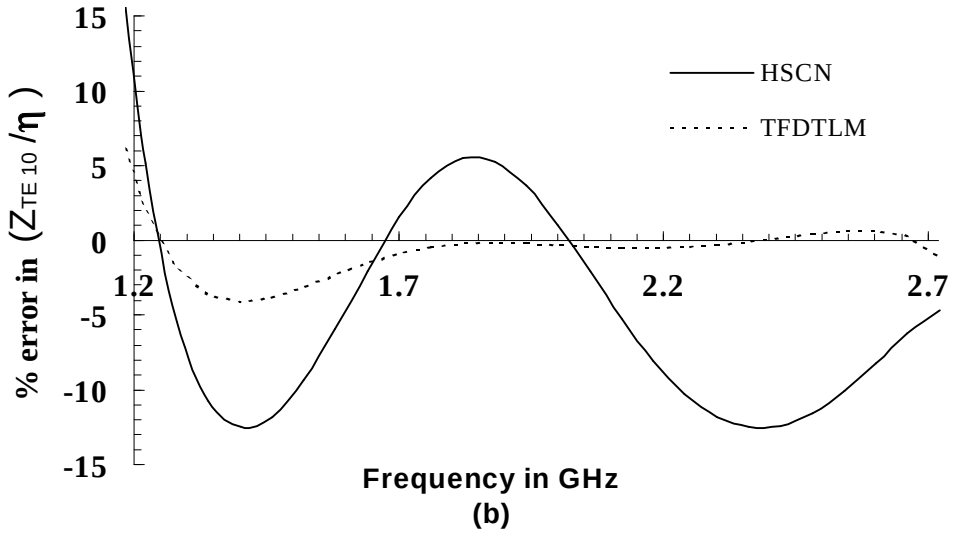

Figure 5.7 Comparison between HSCN II and FDTLM in simulating a rectangular waveguide $\varepsilon_r = 10$ a- $|Z_{TE10}/\eta|$ b- % error in Z_{TE10}/η after cutoff

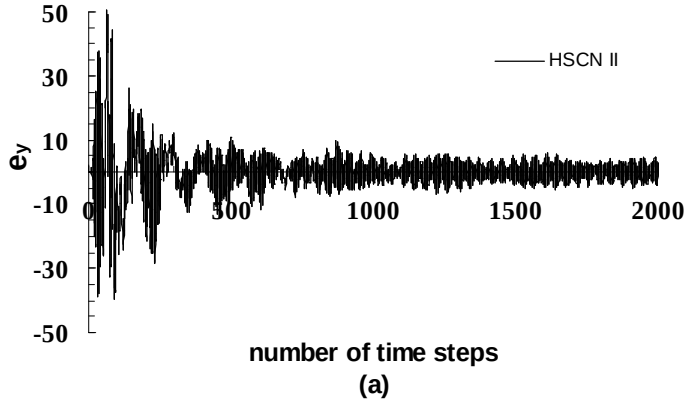

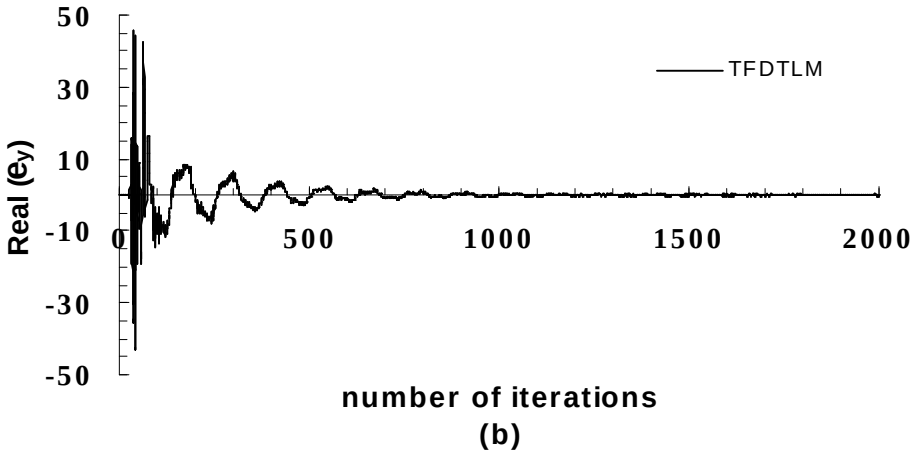

Figure 5.8 Simulation of a waveguide with $\varepsilon_r = 10$
a - Time domain response of the e_y component in the HSCN II
b - Real part of e_y versus number of iterations in the TFDTLM

Figure (5.7a-b) show similar results to those in (5.6a-b) but with ε_r =10. From Figure (5.7b), it appears that the behavior of a traditional time domain TLM is significantly degraded for a higher dielectric constant. The error in the impedance calculation after cutoff can reach a maximum of 12.5 % with an average magnitude from 1.25 f_c to 2.8 f_c of about 7.3 %. On the other hand, the error in the TFDTLM is always less than 3.5 % with an average magnitude from 1.25 f_c to 2.8 f_c of about 1.2 %. Surprisingly, the amount of error appears to be even less than that obtained with ε_r = 2. The apparent improved performance of the TFDTLM for higher dielectric constant can be attributed to one interesting property of the TFDTLM. It was observed that when trying to optimize the coefficients of a first order approximation filter for a medium with a relatively high dielectric constant, the optimization algorithm would add a very small artificial damping factor to the medium propagation constant. Although this artificial damping is very small to affect the accuracy of the approximated propagation factor, it seems that it has an important advantage. This artificial damping would help improve the stability of the absorbing boundary condition which makes it possible to consider a larger number of iterations and consequently higher frequency resolution and more accurate results. The improved stability of the absorbing boundary condition can be observed by comparing the time domain response of the e_y component obtained by the HSCN to the real part of e_y versus iterations obtained from the TFDTLM as shown in Figure (5.8a-b).

5.3 Simulation of waveguide bandpass filter

In this section, a waveguide bandpass filter is simulated. The filter is formed of an infinitely long section of a rectangular waveguide structure loaded at specific locations with lossless obstacles. The obstacles considered here are assumed to be zero thickness symmetrical inductive irises. The structure is shown in Figure (5.9a). The structure can be modeled by transmission line sections of the appropriate length, characteristic impedance equal to the intrinsic impedance of the propagating mode (assuming only the dominant TE_{10} mode is propagating) and propagation factor equal to that of the propagating mode. The obstacles are modeled by shunt elements. The modal expansion method is used to obtain formulas for the admittance values of these shunt elements. These formulas are in the form of integral equations which are solved using the method of moments [29]. The derivation of the equivalent shunt element of an inductive iris is shown in Appendix B. Once the equivalent shunt element is calculated, the whole structure will have a determined equivalent circuit model shown in Figure (5.9b). The S - parameters can be obtained from the equivalent circuit and used as a reference. The waveguide has a = b =5 cm. A second order Higdon's absorbing boundary condition is used for the transverse planes at z = 0 and z = 10 to simulate an infinitely extended waveguide. The irises dimensions and locations are shown in Figure (5.9b). The observation point is chosen somewhere in the middle between the second iris and the absorbing boundary. Two cases will be considered, In the first one, the bandpass filter is assumed to be lossless filled with some dielectric. The S_{21} is then calculated from both the HSCN II and the TFDTLM and the results are compared to that obtained from the equivalent circuit model. In

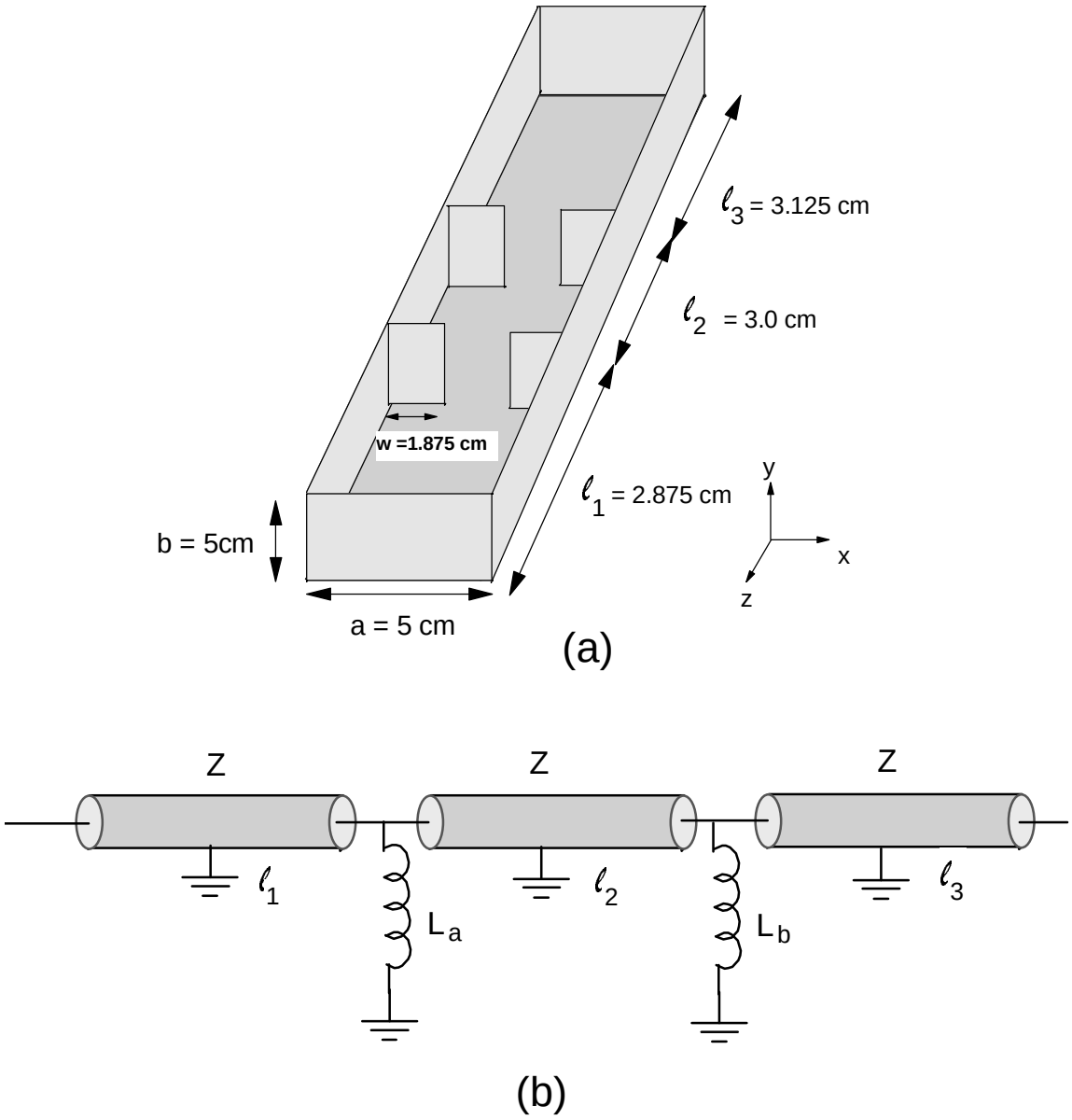

Figure 5.9
a - A waveguide bandpass filter structure b- Equivalent circuit model

the second case, the waveguide is assumed to be filled with a lossy dielectric material.

5.3.1 Simulation of a lossless waveguide bandpass filter

A lossless waveguide bandpass filter is simulated for different dielectric filling. The S_{21} obtained from both the HSCN II and the TFDTLM is compared to that obtained from modal analysis and equivalent circuit model. In the TFDTLM, a first order filter approximation is used with the same assumptions in section 5.2. The only difference is that in this case a finer grid is used to be able to accurately model the irises. In all the following waveguide bandpass filter simulations, a uniform cell is considered with dx = dy = dz $= 2\Delta\ell_1$ =0.25 cm. Again the filter coefficients are optimized over a frequency range where the cell dimension is less than or equal to 0.125 times the corresponding wavelength.

Figure (5.10) shows the S_{21} of the bandpass filter obtained from the HSCN versus that obtained from modal analysis and circuit model. Figure (5.11) shows the corresponding result obtained from the TFDTLM. Comparing the two figures, it becomes obvious that the TFDTLM is able to provide better accuracy than the HSCN. The actual bandwidth obtained from modal analysis and equivalent circuit modal is 31.3 MHz. The bandwidth obtained by the HSCN was found to be 27.5 MHz with a percentage error of about 12 %. On the other hand,

that the bandwidth obtained by the TFDTLM was found to be 33 MHz with an error of only 5 %. Table 5.3 summarizes the above results

Table 5.3 Comparison of the error in bandwidth obtained from the TFDTLM, the HSCN and equivalent circuit model in the simulation of a waveguide bandpass filter with $\varepsilon_r = 6$

Actual	Bw = 31.3 MHz	% error
HSCN	27.5 MHz	-12 %
TFDTLM	33 MHz	5 %

Figure (5.12) and (5.13) show similar results to those in (5.10) and (5.11) but with a relative dielectric constant of 10. Figure (5.12) shows that the behavior of the HSCN II is significantly degraded. On the other hand Figure (5.13) shows that the S_{21} obtained from the TFDTLM is almost in perfect match with that obtained from modal analysis. The apparent improved accuracy of the TFDTLM can be attributed to the same reason discussed in section 5.2.

Another good reason for the absorbing boundary to perform better with the TFDTLM than with the HSCN is the following : the absorbing boundary is designed to absorb a wave in a medium with some dielectric constant ε_r. In the HSCN, the delay along the link lines is equal to that in free space and the extra delay is compensated through the use of stubs

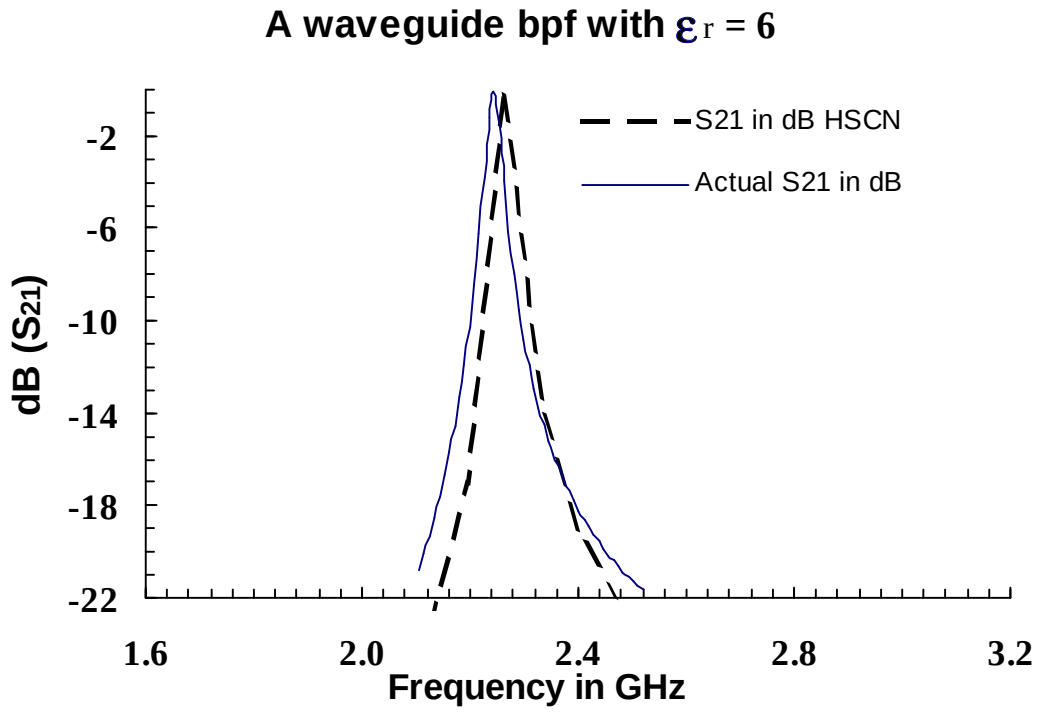

Figure 5.10 S_{21} Obtained from the HSCN II versus that obtained from modal analysis and circuit model in the simulation of a waveguide bandpass filter with $\varepsilon_r = 6$

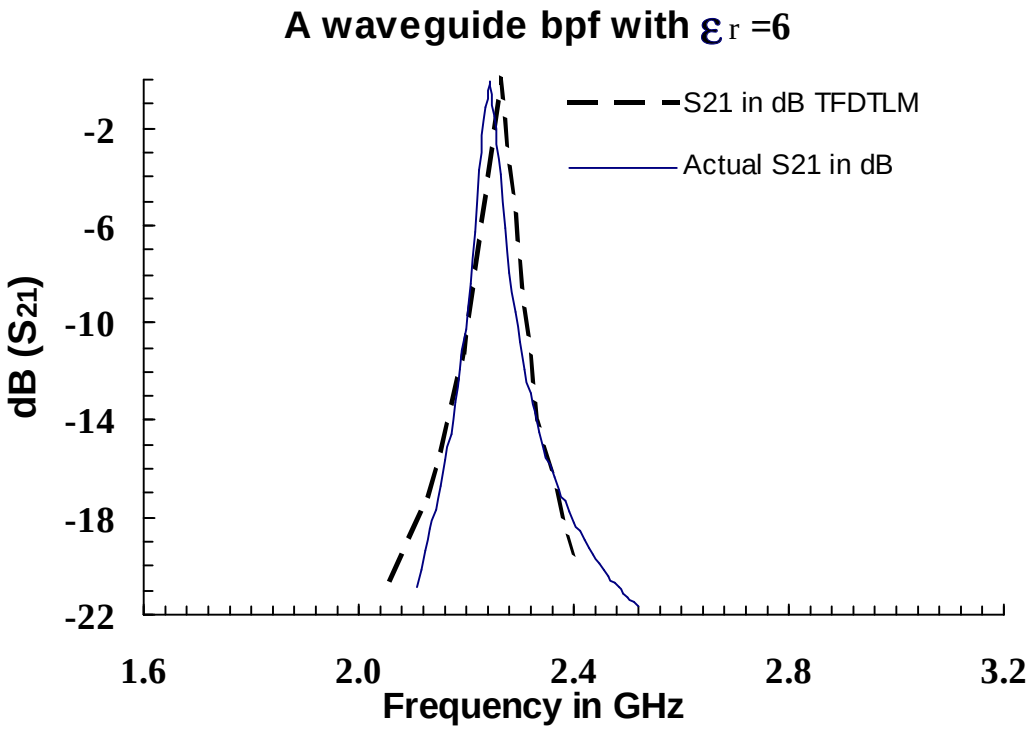

Figure 5.11 S_{21} Obtained from the TFDTLM versus that obtained from modal analysis and circuit model in the simulation of a waveguide bandpass filter with $\varepsilon_r = 6$

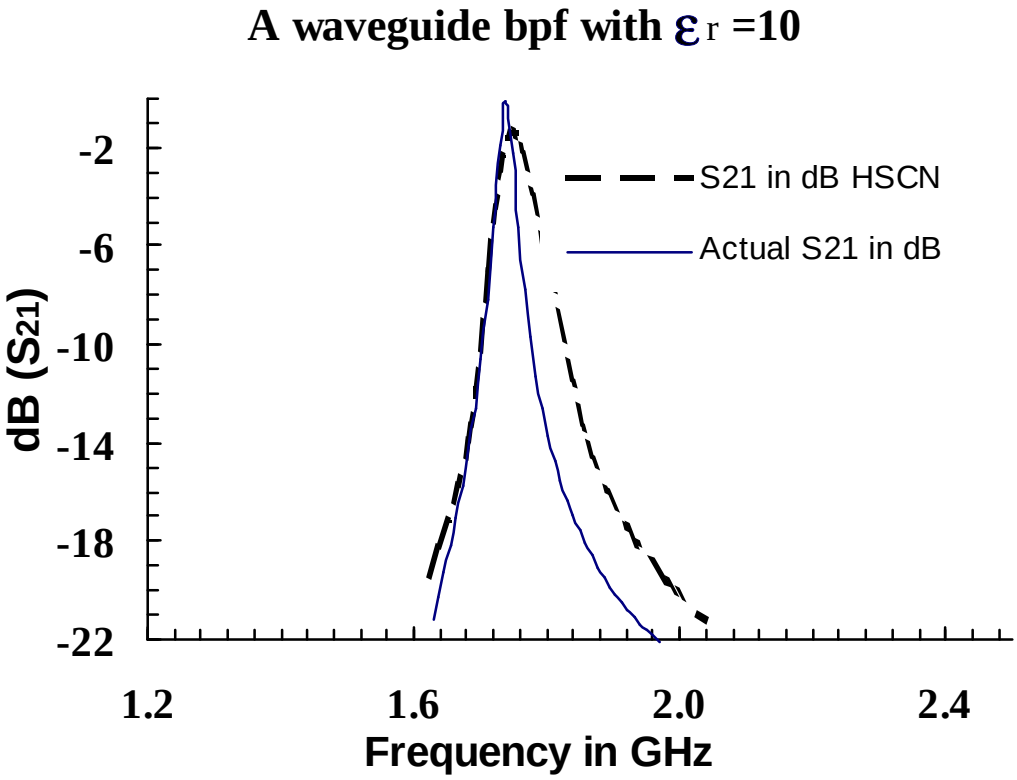

Figure 5.12 S_{21} Obtained from the HSCN versus that obtained from modal analysis and circuit model in the simulation of a waveguide bandpass filter with $\varepsilon_r = 10$

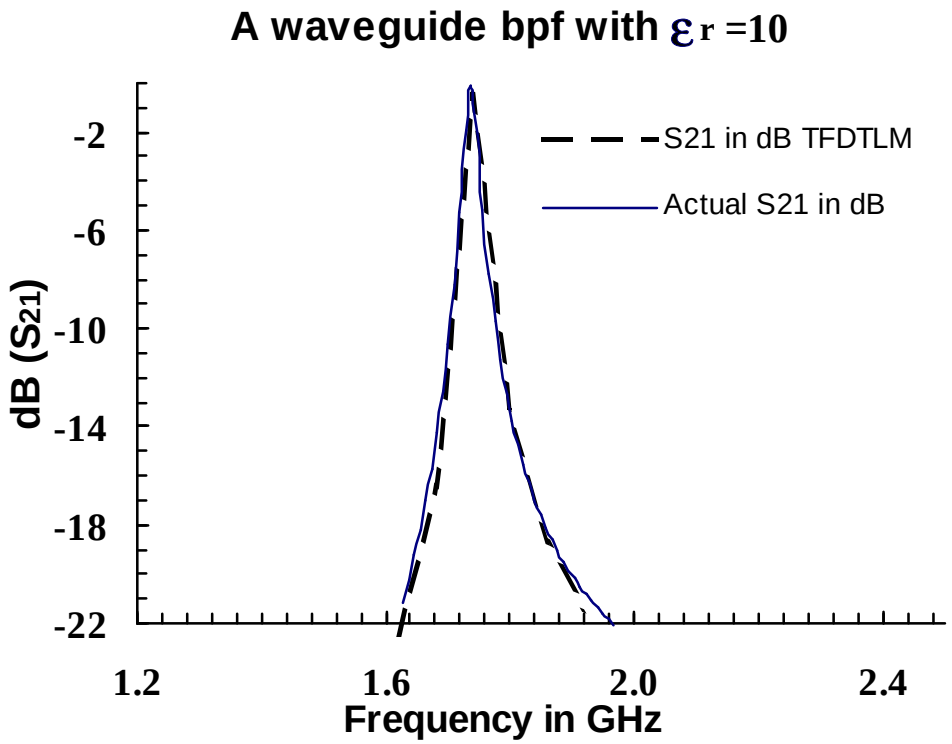

Figure 5.13 S_{21} Obtained from the TFDTLM versus that obtained from modal analysis and circuit model in the simulation of a waveguide bandpass filter with $\varepsilon_r = 10$

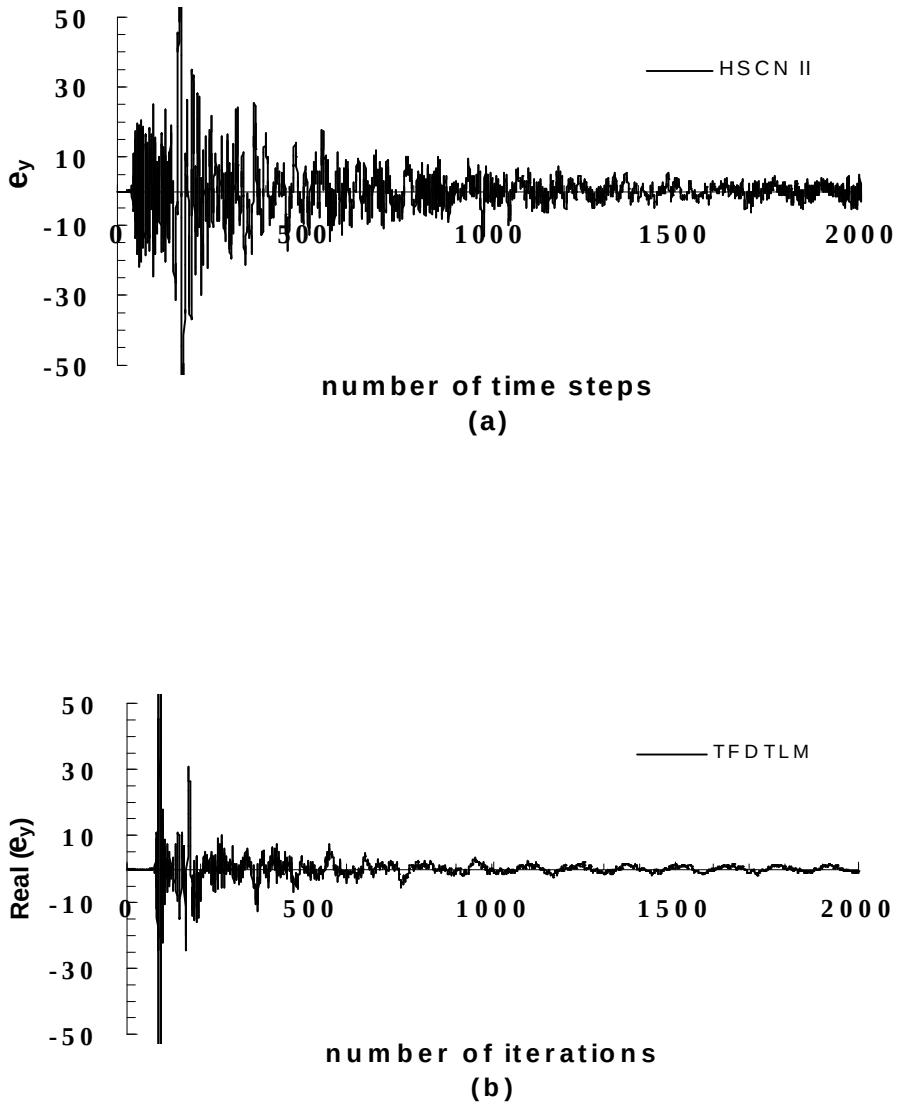

Figure 5.14 Simulation of a waveguide bandpass filter with $\varepsilon_r = 10$
a - Time domain response of the e_y component in the HSCN II
b - Real part of e_y versus number of iterations in the TFDTLM

concentrated at the nodes centers. The fact that the speed of propagation along the link lines is different from the speed of the wave the boundary is designed to absorb creates some type of discontinuity or mismatch. This mismatch help degrade the quality of absorption. In the TFDTLM, on the other hand, although the delay or propagation factor is being approximated by a filter, the fact that its being distributed along the link line help get rid of the discontinuity inherent in the HSCN. Figure (5.14a-b) demonstrates the improved performance of the same absorbing boundary condition with the TFDTLM than with HSCN. Figure (5.14a) shows the time domain response of the bandpass filter with for $\varepsilon_r = 10$ obtained by the HSCN. Figure (5.14b) shows the real part of the field component e_y versus the number of iterations obtained by the TFDTLM.

5.3.2 Simulation of a lossy waveguide bandpass filter

A lossy waveguide bandpass filter is simulated. The waveguide is filled with a lossy material having a relative dielectric constant equal to 6 . The S_{21} obtained from both the HSCN II and the TFDTLM are compared to that obtained from modal analysis and equivalent circuit model for different conductivities of the dielectric filling. In the TFDTLM, a second order filter approximation is used. The filter is denoted by F_2 and has the form

$$F_2 = e^{-\gamma_1 \Delta l_1}\left(\frac{a_0 + a_1 e^{-\gamma_1 \Delta l_1} + a_2 e^{-2\gamma_1 \Delta l_1}}{b_0 + b_1 e^{-\gamma_1 \Delta l_1} + b_2 e^{-2\gamma_1 \Delta l_1}}\right) \tag{5.2}$$

The cell dimensions are chosen as in section 5.3.1. Again the filter coefficients are optimized over a frequency range where the cell dimension is less than or equal to 0.125 times the corresponding wavelength.

Figure (5.15) shows the S_{21} of the bandpass filter obtained from the HSCN versus that obtained from modal analysis and circuit model for a conductivity of 0.06 s/m. Figure (5.16) shows the corresponding result obtained from the TFDTLM. Comparing the two figures, it becomes obvious that the TFDTLM is able to provide better accuracy than the HSCN. The same conclusion derived from the simulation of a lossy cavity can be observed here. The HSCN overestimates the quality factor of the filter which can be attributed to its inability to accurately model the medium losses. The actual quality factor obtained from modal analysis and equivalent circuit modal is 11. The quality factor obtained by the HSCN was found to be 24.4 with a percentage error of over a 100 %. On the other hand, that the quality factor obtained by the TFDTLM was found to be 10.3 MHz with an error of only 6 %.

Figure (5.17) and (5.18) show similar results to those in (5.15) and (5.16) but with a higher loss tangent, here the conductivity is taken to be 0.1 s/m . Figure (5.17) shows that the behavior of the HSCN II is significantly degraded. On the other hand Figure (5.18) shows that the S_{21} obtained from the TFDTLM is in quite good agreement with that obtained from

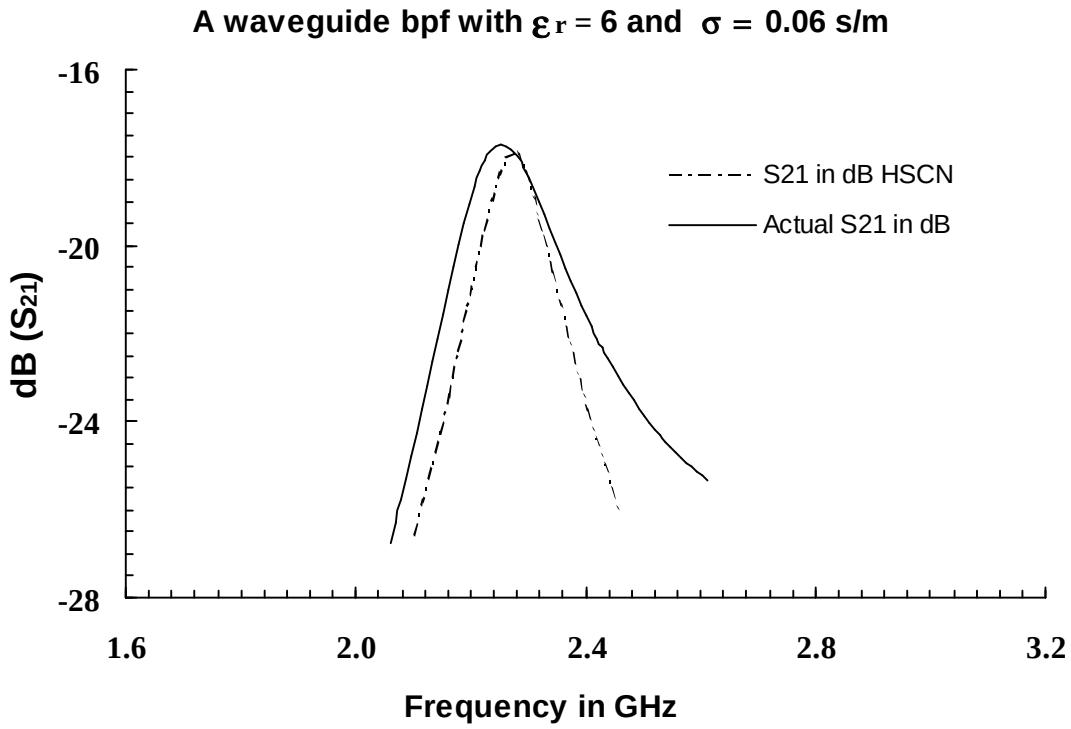

Figure 5.15 S_{21} Obtained from the HSCN versus that obtained from modal analysis and circuit model in the simulation of a waveguide bandpass filter with $\varepsilon_r = 6$, $\sigma = 0.06$ s/m

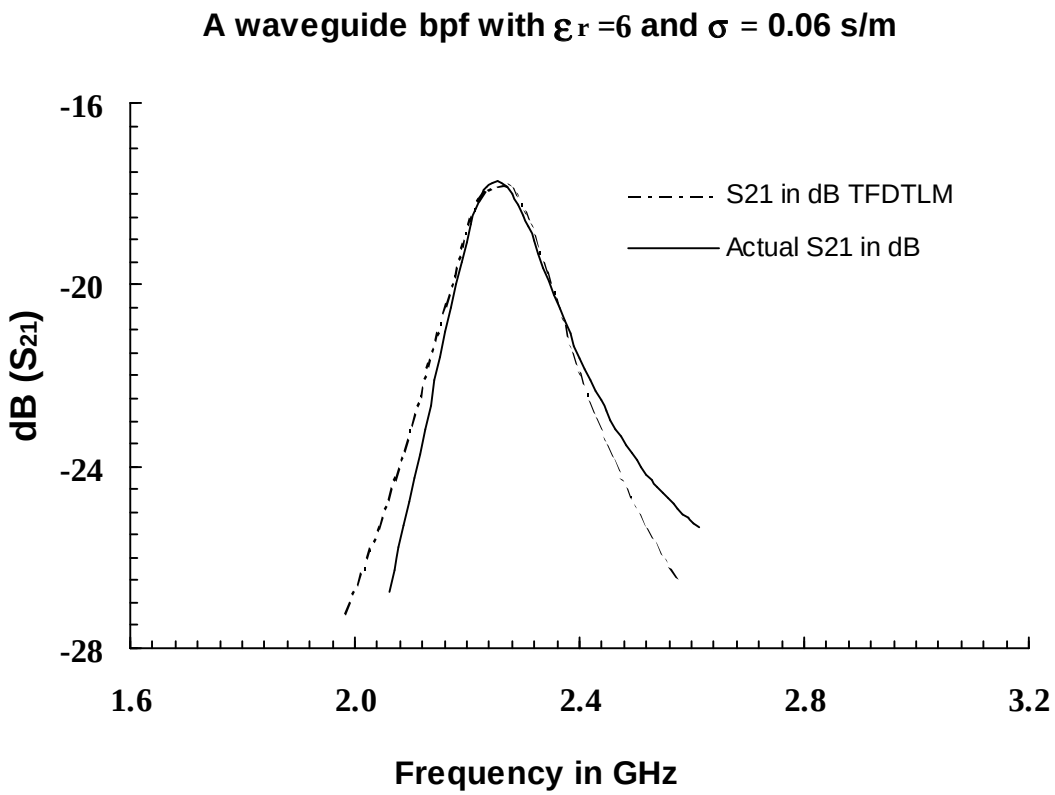

Figure 5.16 S_{21} Obtained from the TFDTLM versus that obtained from modal analysis and circuit model in the simulation of a waveguide bandpass filter with $\varepsilon_r = 6$, $\sigma = 0.06$ s/m

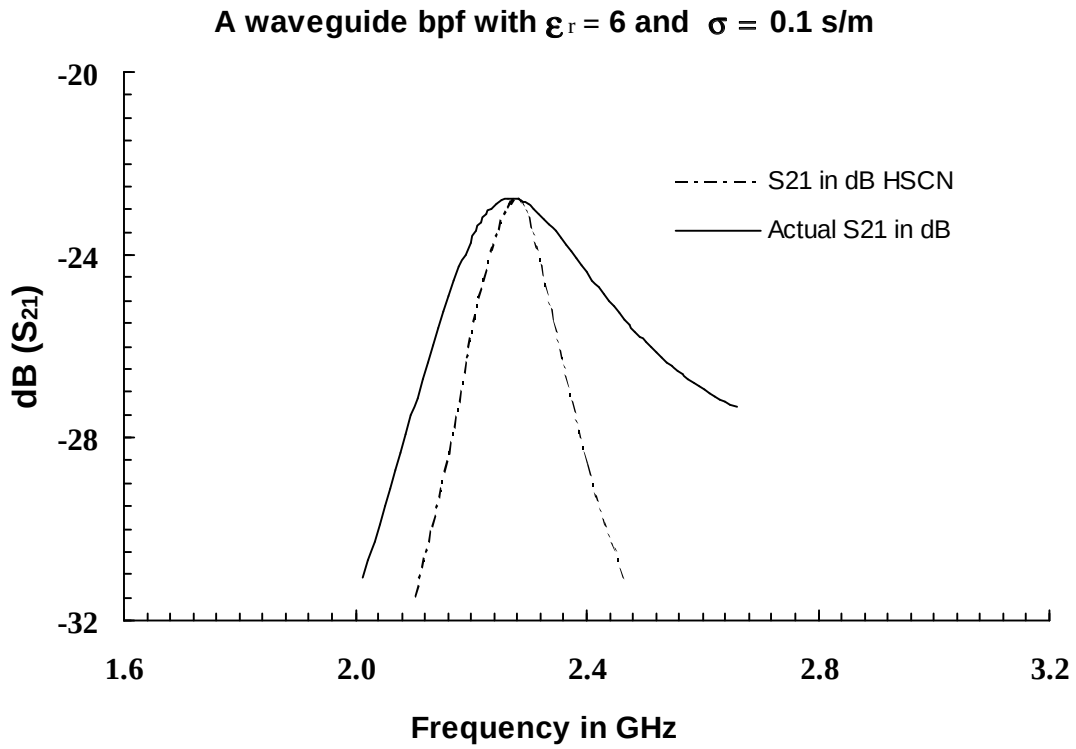

Figure 5.17 S_{21} Obtained from the HSCN versus that obtained from modal analysis and circuit model in the simulation of a waveguide bandpass filter with $\varepsilon_r = 6$, $\sigma = 0.1$ s/m

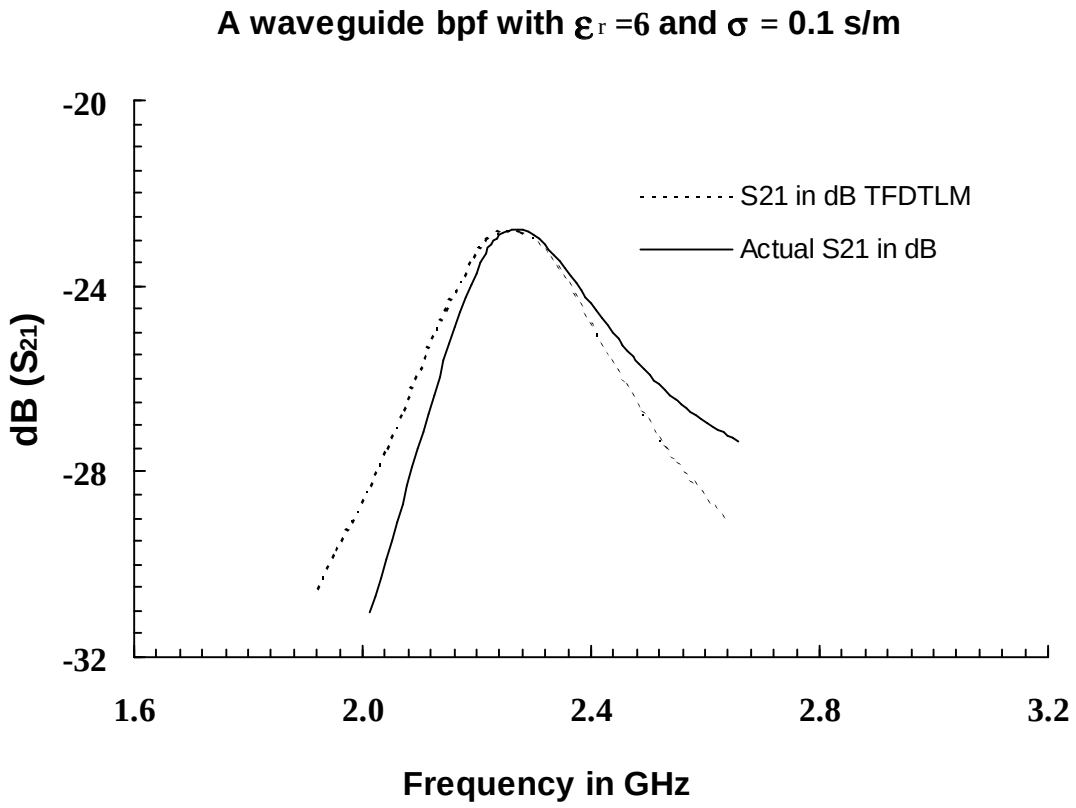

Figure 5.18 S_{21} Obtained from the TFDTLM versus that obtained from modal analysis and circuit model in the simulation of a waveguide bandpass filter with $\varepsilon_r = 6$, $\sigma = 0.1$ s/m

modal analysis.

5.4 Summary

In this chapter, the TFDTLM was implemented in a three dimension mesh. Some structures were simulated and the ability of the TFDTLM to accurately model wave propagation in lossy inhomogeneous media was demonstrated. These structures included a cavity, a waveguide and waveguide bandpass filter. First order approximation filters were used for lossless inhomogeneous media while second order approximation filters were used for lossy inhomogeneous medium.

The TFDTLM was able to provide more accurate results as compared to the HSCN. Furthermore, the behavior of the HSCN was found to be significantly degraded as the relative dielectric constant and/or the loss tangent are increased. The TFDTLM, on the other hand, almost maintained the same order of accuracy with increased relative dielectric constant and/or loss tangent.

Another important advantage of the TFDTLM that was also revealed from the simulation, is that it can easily be interfaced with any of the absorbing boundary conditions originally developed for time domain TLM with the slightest modifications. The absorbing boundary was found to perform even better with the TFDTLM than with a time domain TLM for reasons discussed earlier.